
MODELING CENSORED MOBILITY DEMAND THROUGH QUANTILE REGRESSION NEURAL NETWORKS

A PREPRINT

Inon Peled, Filipe Rodrigues, Francisco C. Pereira

April 6, 2021

ABSTRACT

Shared mobility services require accurate demand models for effective service planning. On one hand, modeling the full probability distribution of demand is advantageous, because the full uncertainty structure preserves valuable information for decision making. On the other hand, demand is often observed through usage of the service itself, so that the observations are *censored*, as they are inherently limited by available supply. Since the 1980s, various works on Censored Quantile Regression models have shown them to perform well under such conditions, and in the last two decades, several works have proposed to implement them flexibly through Neural Networks (CQRNN). However, apparently no works have yet applied CQRNN in the Transport domain. We address this gap by applying CQRNN to datasets from two shared mobility providers in the Copenhagen metropolitan area in Denmark, as well as common synthetic baseline datasets. The results show that CQRNN can estimate the intended distributions better than both censorship-unaware models and parametric censored models.

1 Introduction

Shared mobility services – e.g., taxis, bike-sharing and ridesourcing – offer several socio-economic benefits, such as reduced emissions, less traffic congestion and less need for parking (Santos, 2018, Smith and Hensher, 2020). Effective planning and deployment of such services require reliable estimates of mobility demand, as also obtainable from data-driven modeling (Laporte et al., 2018, Profillidis and Botzoris, 2019).

The data used in demand modeling is often derived from observations of service usage, which are thus inherently limited by available vehicle supply. Moreover, the data of any mobility service provider does not account for demand lost to competing services and other transport modes. Consequently, actual demand for mobility is typically latent (i.e., unknown) and its observations are likely to lie below it, namely, they are often *right-censored*.

A joint work with Gammelli et al. (2020) shows that censorship-aware models can better estimate latent mobility demand, thereby allowing service providers to make better informed decisions. The models in that work are based on censored Gaussian Processes, which yield a full distribution of latent demand. However, while Gaussian Processes allow for a flexible, non-parametric fit, they still impose a Gaussian assumption on the latent distribution, and they also face some limitations when scaling to big datasets.

In this work, we propose to model latent mobility demand via Censored Quantile Regression Neural Networks (CQRNN), which are also non-parametric, yet do not face the aforementioned limitations. CQRNN estimates quantiles of the latent distribution via Neural Networks while accounting for censorship in the observed demand. We empirically demonstrate the advantages of CQRNN on synthetic datasets and apply CQRNN to demand estimation in real-world shared mobility data.

To the best of our knowledge, this is the first work to apply Censored Quantile Regression Neural Networks in the Transport domain. Furthermore, whereas existing works on CQRNN often assume fixed censorship, we conduct experiments with dynamic, random censorship. We also provide the Python implementation of our CQRNN models in <https://github.com/inon-peled/cqrnn-pub/>.

The rest of this work is organized as follows. In Section 4.1, we review works related to CQRNN and identify knowledge gaps, particularly in the Transport domain. Section 3 then describes our CQRNN methodology, and we demonstrate its advantages via experiments on synthetic data in Section 4. In Section 5, we apply our methodology to censored datasets from two shared mobility services in Denmark: bike-sharing and shared Electric Vehicles. Finally, Section 6 summarizes our findings and outlines our future work plans.

2 Literature Review

In this Section, we review existing works on non-censored and censored Quantile Regression (QR), and in particular, Neural Network-based QR. For the more general topics of Censored Regression and Neural Networks, we kindly refer the reader to the following resources. A review of censored and non-censored methods for mobility demand modeling appears in our recent joint work with Gammelli et al. (2020). The general theory and practice of Neural Networks is well studied in (Nielsen, 2015), and several of their recent applications in the transport domain are reviewed in (Himanen et al., 2019).

Let us first introduce the general method of Quantile Regression (Koenker and Bassett, 1978), regardless of censorship. For any probability distribution and $0 < \theta < 1$, the θ 'th *quantile* is the smallest value at which the cumulative probability mass is θ . QR approximates a latent distribution by estimating its quantiles for given θ 's, and thus does not presume any parametric form for the distribution. The regression itself can follow any functional form – e.g., linear (Koenker and Bassett, 1978), nonlinear (Koenker and Park, 1996), multivariate (Carlier et al., 2016) or nonparametric (Zheng, 2012) – and the quantiles can be combined into a fully estimated distribution (Cannon, 2011, Quiñonero-Candela et al., 2006).

Importantly, the fully estimated distribution preserves useful information, which might otherwise be lost through the more common practice of estimating only a few central moments, such as mean and standard deviation (Peled et al., 2019). In turn, the preserved information allows for better informed decisions, e.g., service operators can use the full uncertainty structure of future demand to decide whether to balance the fleet conservatively or more opportunistically. In addition, by taking values of θ close to 0 and 1, QR can be more robust to outliers than mean regression (Koenker, 2005).

A variant of QR is Censored Quantile Regression (CQR), where observed realizations from a latent distribution are assumed to be clipped at some thresholds. The distribution of these observations is then a mixture of continuous (within the observable range) and discrete (at each threshold). Many works on CQR build upon the early formulation by Powell (1984, 1986), as we ultimately do too in Section 3. Some of these works focus on estimators of derived CQR formulations (Buchinsky, 1998, Cheng and Tzeng, 2014, Chernozhukov et al., 2015, Galvao et al., 2013, Leng and Tong, 2013). Others works on CQR develop more complex and non-parametric models, as we next review, starting with models that are not based on Neural Networks.

Yu and Stander (2007) devise a Bayesian Inference approach to linear CQR, in which they use the Asymmetric Laplace likelihood, as also common in other Bayesian CQR works (Yang et al., 2016). They evaluate their approach on some commonly used, censored data baselines: synthetic datasets, which we too use in Section 4, and a real-world dataset of women's labor force participation (Mroz, 1987). Gannoun et al. (2005) develop a CQR model based on local linear approximations and evaluate it on synthetically generated datasets. Shim and Hwang (2009) offer a Support Vector Machine-based CQR model, which they evaluate on the same synthetic datasets as in Gannoun et al. (2005), and on a real-world dataset of heart transplant survival. Li and Bradic (2020) propose a Random Forest-based CQR model, which they compare with other Random Forest models on both synthetic data and two real-world datasets: housing prices and a biliary disease.

In the last two decades, Neural Networks have increasingly been used for Quantile Regression (QRNN) in multiple research areas, taking advantage of their flexible, nonlinear modeling capabilities. For non-censored regression, Taylor (2000) provides an early form of QRNN with a single dense hidden layer, and uses it to estimate a latent distribution of multiperiod financial returns. In studies of the electric power industry, He et al. use non-censored QRNN to estimate latent distributions of electricity production (He and Li, 2018, He and Zhang, 2020) and consumption (He et al., 2019), while Haben and Giasemidis (2016) and Zhang et al. (2018) use non-censored QRNN to predict electricity loads. In the Transport domain, (Tian et al., 2020) use a non-censored QRNN with a single hidden neuron to predict 15 min air traffic in a Chinese airport, and Rodrigues and Pereira (2020) devise a non-censored, multi-output QRNN that jointly estimates mean and quantiles, whereby they predict 30 min taxi demand in New York City.

Very few works apply QRNN in a Censored setting (CQRNN). Cannon (2011) develops a general architecture for both censored and non-censored QRNN, which he implements as an R package. He uses a smoothing technique by Chen (2007) to replace the loss function with a differentiable approximation, which is amenable to gradient-based training,

and applies the implementation in a censored case study of precipitation forecasting. Jia and Jeong (2020) propose another CQRNN model, similar to but deeper than that of (Cannon, 2011). They implement their model in Python via Keras and apply it to censored survival datasets: a synthetic dataset and a breast cancer dataset.

Except for (Cannon, 2011) and (Jia and Jeong, 2020), we are not aware of other works that use Quantile Regression Neural Networks in Censored case studies. In particular, there appear to be no works on CQRNN in the transport domain, despite the prevalent censorship in transport data (Section 1), the flexibility of Neural Networks and the advantages of Quantile Regression. We next address this gap by applying CQRNN to several datasets of real-world shared mobility services.

3 Methodology

A censored dataset consists of covariates $\mathbf{x}_1, \dots, \mathbf{x}_N$ and corresponding observations y_1, \dots, y_N , which are clipped versions of latent variables y_1^*, \dots, y_N^* . Namely, for some thresholds τ_1, \dots, τ_N , all the observations are either left-censored or right-censored, such that:

$$y_i = \begin{cases} y_i^*, & y_i^* > \tau_i \\ \tau_i, & y_i^* \leq \tau_i \end{cases} \text{ in left-censorship,} \quad (1)$$

$$y_i = \begin{cases} y_i^*, & y_i^* < \tau_i \\ \tau_i, & y_i^* \geq \tau_i \end{cases} \text{ in right-censorship.} \quad (2)$$

Each threshold is either given or unknown, and if censorship is fixed, then $\tau_1 = \dots = \tau_N$. y_1^*, \dots, y_N^* are drawn from a latent distribution, whose θ 'th quantiles we wish to estimate for some $0 < \theta < 1$. To this end, we construct, fit and evaluate various Neural Networks (NNs), as follows.

We construct NNs independently for each θ 'th quantile, as illustrated in Figure 1. All the NNs are Feed-Forward and optionally use input Dropout (Srivastava et al., 2014) for regularization. Throughout the experiments, we vary the Hidden layers and the activation function of the Aggregate Outputs layer. To experiment with right-censored datasets, we also negate each NN input and output as well as mirror the output quantiles, e.g., swap the output for $\theta = 0.05$ with the output for $\theta = 0.95$.

Fitting is done by minimizing a dedicated loss function, which we next describe. As mentioned in Section 2, Yu and Stander (2007) use the following likelihood function for Bayesian Inference with left-censorship at zero:

$$\mathcal{S} \left(y_1^{(j)}, \dots, y_N^{(j)} \mid \boldsymbol{\beta}^{(j)}, \mathbf{x}_i, \theta \right) = \theta^N (1 - \theta)^N \exp \left\{ - \sum_{i=1}^N \rho_\theta \left(y_i - \max \left\{ 0, \mathbf{x}_i^\top \boldsymbol{\beta}^{(j)} \right\} \right) \right\}, \quad (3)$$

where $\rho : \mathbb{R} \rightarrow \mathbb{R}$ is the Tilted Loss (TL) function,

$$\rho_\theta(r) = \max\{\theta r, (\theta - 1)r\}. \quad (4)$$

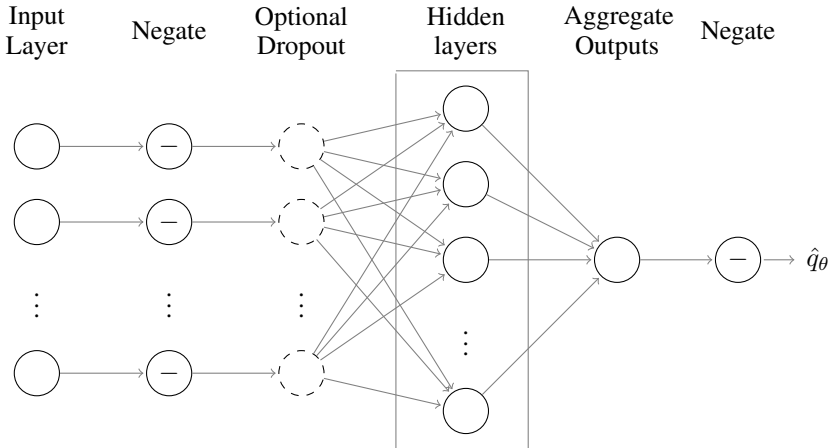


Figure 1: Our Censored Quantile Regression Neural Network architecture.

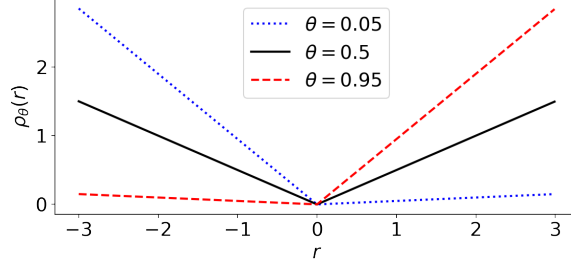


Figure 2: Tilted Loss.

Figure 2 illustrates how TL penalizes the prediction error $r = \hat{q}_\theta - y$ in a manner that depends on θ . For the median ($\theta = 0.5$), the loss is the same regardless of the sign of r . For quantiles above the median (e.g., $\theta = 0.95$), the loss is worse for $y > \hat{q}_\theta$ than for $y < \hat{q}_\theta$ with the same magnitude of r , and vice versa for quantiles below the median (e.g., $\theta = 0.05$). For any θ , the loss equals zero if $y = \hat{q}_\theta$ and is otherwise positive.

Based on (3), we use the following likelihood function:

$$\mathcal{C} \left(y_1^{(j)}, \dots, y_N^{(j)} \mid \boldsymbol{\beta}^{(j)}, \mathbf{x}_i, \theta \right) = \theta^N (1 - \theta)^N \exp \left\{ - \sum_{i=1}^N \rho_\theta \left(y_i - \max \{ \tau_i, \hat{q}_{\theta,i} \} \right) \right\}, \quad (5)$$

where $\hat{q}_{\theta,i}$ is the NN output; note that τ_i must be specified also for non-censored observations. The Negative Log-Likelihood (NLL) of (5) is the loss function for fitting.

We fit each NN using backpropagation and the Adam optimizer (Kingma and Ba, 2014) with norm clipping at 1, while using a validation set for early stop. For hyper-parameter optimization, we experiment with Adam learning rates in $\{0.001, 0.01, 0.1, 1\}$, and choose the one that performs best on the validation set. Additional details about architecture, initialization, fitting and evaluation depend on the dataset and manner of experimentation, as in the following Sections.

4 Experiments for Demonstrating the Advantages of Censored Quantile Regression

In this Section, we empirically demonstrate some advantages of Censored Quantile Regression Neural Networks (CQRNN). First, we compare CQRNN with censorship-unaware Quantile Regression and show that CQRNN can better reconstruct latent values. Then, we compare CQRNN to parametric Censored Regression and show an advantage and disadvantage of each modeling method. The experiments in this Section are based on commonly used, synthetic baseline datasets, and the next Section proceeds to use real-world transport datasets.

4.1 Non-censored vs. Censored Quantile Regression

Let us first show that the predictive quality of Quantile Regression Neural Networks can improve by accounting for data censorship. For this, we use some common synthetic baseline datasets, as in Yu and Stander (2007), where the latent variable is

$$y^* = x_0 + x_1 + x_2 + \varepsilon, \quad (6)$$

where $x_0 = 1, x_1 \in \{-1, 1\}, x_2 \in \mathbb{R}$ and the noise ε follows some distribution with 0 mean. Left-censorship occurs at zero, so that we observe

$$y = \max\{0, y^*\}. \quad (7)$$

For any random variable A and $0 < \theta < 1$, let $q_\theta(A|\mathbf{x})$ denote the θ 'th conditional quantile of A given $\mathbf{x} = [x_0, x_1, x_2]^\top$. Hence:

$$q_\theta(y|\mathbf{x}) = \max\{0, q_\theta(y^*|\mathbf{x})\} = \max\{0, x_0 + x_1 + x_2 + q_\theta(\varepsilon|\mathbf{x})\}. \quad (8)$$

Similarly to (Yu and Stander, 2007), we experiment with $\theta = 0.05, 0.50, 0.95$ and three noise distributions,

$$\text{Standard Gaussian: } \varepsilon^{(1)} \sim \mathcal{N}(0, 1), \quad (9)$$

$$\text{Heteroskedastic: } \varepsilon^{(2)} \sim (1 + x_2)\mathcal{N}(0, 1), \quad (10)$$

$$\text{Gaussian Mixture: } \varepsilon^{(3)} \sim 0.75\mathcal{N}(0, 1) + 0.25\mathcal{N}(0, 2^2). \quad (11)$$

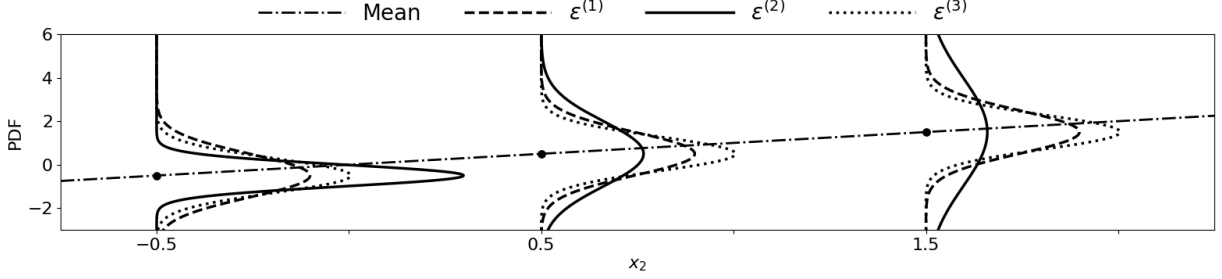


Figure 3: Distribution of synthetic y^* for $x_0 = 1, x_1 = -1, x_2 = -0.5, 0.5, 1.5$ and each noise distribution $\varepsilon^{(j)}$. In each case, y^* follows a Gaussian distribution with mean $x_0 + x_1 + x_2$ (dash-dotted line). For the Standard Gaussian noise (dashed) and Gaussian Mixture noise (solid), the distribution of y^* is homoskedastic, i.e., has fixed variance 1 and 0.791^2 , respectively. For the Heteroskedastic noise (dotted), y^* has variance that changes with x_2 as $(1 + x_2)^2$.

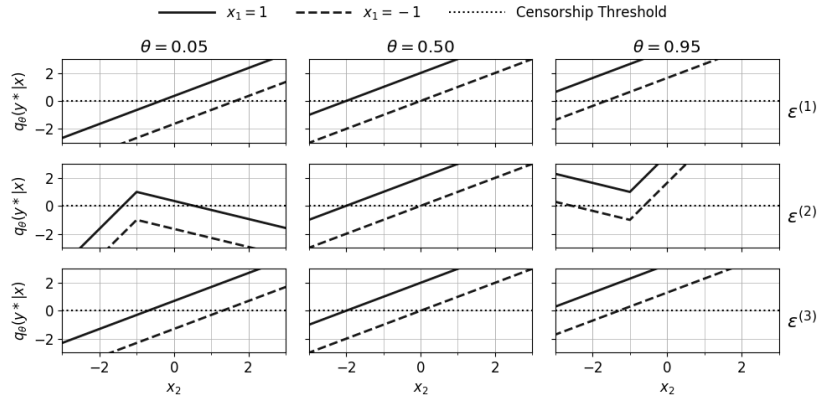


Figure 4: Conditional quantiles of synthetic y^* for each noise distribution.

The corresponding conditional quantiles of y are thus

$$q_\theta \left(y^{(j)} | \mathbf{x} \right) = \max \left\{ 0, q_\theta \left(y^{*,j} | \mathbf{x} \right) \right\}, \quad (12)$$

such that:

$$q_\theta \left(y^{*,1} | \mathbf{x} \right) = \Phi^{-1} \left(x_0 + x_1 + x_2, 1 \right), \quad (13)$$

$$q_\theta \left(y^{*,2} | \mathbf{x} \right) = \Phi^{-1} \left(x_0 + x_1 + x_2, |1 + x_2| \right), \quad (14)$$

$$q_\theta \left(y^{*,3} | \mathbf{x} \right) = \Phi^{-1} \left(x_0 + x_1 + x_2, \sqrt{0.75^2 + 0.25^2} \right), \quad (15)$$

where $\Phi^{-1}(\mu, \sigma) : [0, 1] \rightarrow \mathbb{R}$ is the quantile function of $\mathcal{N}(\mu, \sigma^2)$. Figure 3 illustrates the distribution of y^* with each noise, for $x_1 = 1$ and several values of x_2 . Figure 4 illustrates the conditional quantiles of y^* for each noise and θ . For Heteroskedastic noise, the conditional quantiles of y^* are non-linear, as their slopes change at $x_2 = -1$.

For each $\varepsilon^{(j)}$, $j = 1, 2, 3$, we generate a synthetic dataset by independently drawing $N = 1000$ samples from $\varepsilon^{(j)}$ and \mathbf{x} , where

$$x_0 = 1, \quad x_1 \sim \mathcal{U}\{-1, 1\}, \quad x_2 \sim \mathcal{N}(0, 1). \quad (16)$$

We then also compute the corresponding y^* and y , and obtain that approximately 30% of the observations $y_1^{(j)}, \dots, y_N^{(j)}$ are censored. Further, for each θ , Table 1 on the following page provides the percent of zeros among the conditional quantiles $q_\theta(y_1^{(j)} | \mathbf{x}_1^{(j)}), \dots, q_\theta(y_N^{(j)} | \mathbf{x}_N^{(j)})$. The most challenging cases to model are those with $\theta = 0.05$, where the conditional quantiles are particularly prone to censorship.

Dataset	$\theta = 0.05$	$\theta = 0.50$	$\theta = 0.95$
Standard Gaussian	62.7%	23.9%	2.0%
Heteroskedastic	68.0%	23.9%	11.4%
Gaussian Mixture	54.1%	23.9%	4.6%

Table 1: Percent of zero conditional quantiles for the censored observations in each synthetically generated dataset.

For each $j = 1, 2, 3$, we fix train, test and validation sets by randomly partitioning the j 'th dataset as 62% : 15% : 33%, respectively. To model the θ 'th quantile, we use several Neural Networks (NNs), each consisting of a single neuron with activation function η . Namely, each NN takes as input \mathbf{x} and outputs

$$\hat{q}_\theta(y|\mathbf{x}) = \eta(\mathbf{x}^\top \boldsymbol{\beta}), \quad (17)$$

where $\boldsymbol{\beta}$ are trainable weights. We fit each NN on the train set via backpropagation, using Adam optimization with learning rate 0.01 and norm clipping at 1. Weights are initialized to 1, and in each training epoch, the whole train set is processed in a single batch. Training stops when the validation loss does not improve for 10 consecutive epochs.

First, as an example of a common model that ignores censorship, we use a non-censored linear model, where η is the identity function and the loss to be minimized is

$$\rho_\theta(\hat{q}_\theta(y|\mathbf{x}) - y). \quad (18)$$

Next, we turn to censorship-aware models, the first of which is $\mathcal{C}+\Sigma$, where η is the identity function, so that the model is still linear as in (Yu and Stander, 2007). The second censorship-aware model is non-linear, such that η is the Exponential Linear Unit,

$$\text{ELU}(z) = \begin{cases} z, & z > 0 \\ \exp(z) - 1, & z \leq 0 \end{cases}. \quad (19)$$

Finally, we measure the predictive performance of each NN on the test set against the actual conditional quantiles of y^* in Equations (13) to (15). The measures we use are Coefficient of Determination (R^2), Mean Absolute Error (MAE) and Rooted Mean Squared Error (RMSE). For any dataset, these measures are defined as follows, omitting superscripts and function arguments for better legibility:

$$R^2 = 1 - \frac{\sum_{i=1}^N (\hat{q}_{\theta,i} - q_{\theta,i})^2}{\sum_{i=1}^N (\hat{q}_{\theta,i} - \bar{q}_\theta)^2}, \quad \text{MAE} = \frac{1}{N} \sum_{i=1}^N |\hat{q}_{\theta,i} - q_{\theta,i}|, \quad \text{RMSE} = \sqrt{\frac{1}{N} \sum_{i=1}^N (\hat{q}_{\theta,i} - q_{\theta,i})^2}, \quad (20)$$

where \bar{q}_θ is the mean of $q_{\theta,1}, \dots, q_{\theta,N}$. Better predictive quality corresponds to R^2 closer to 1 and MAE and RMSE closer to 0.

The results appear in Table 2 on the next page, which shows that the censorship-aware QRNN models outperform the censorship-unaware model. This holds when evaluating on either the entire test set or its non-censored subset – where the latent values are revealed. For the median ($\theta = 0.5$), the linear CQRNN is mostly the best model, whereas for the more challenging $\theta = 0.05, 0.95$, the non-linear CQRNN is mostly the best model.

4.2 Parametric vs. Non-Parametric Censored Quantile Regression

Since its introduction by Tobin (1958), the Tobit model has become a cornerstone of parametric censored modeling. Tobit assumes that the latent variable depends on covariates linearly with Gaussian white noise, and is censored at a given fixed threshold. Hence in Tobit, the latent quantiles for the i 'th observation are given by the parametric distribution

$$\mathcal{N}(\mathbf{x}_i^\top \boldsymbol{\beta}, \sigma^2), \quad (21)$$

where \mathbf{x}_i are covariates, $\boldsymbol{\beta}$ are linear coefficients to be estimated, and σ is standard deviation, either given or to be estimated too. Further, the Tobit likelihood for upper censorship is

$$\prod_{i=1}^N \left\{ \frac{1}{\sigma} \varphi\left(\frac{y_i - \mathbf{x}_i^\top \boldsymbol{\beta}}{\sigma}\right) \right\}^{1-l_i} \left\{ 1 - \Phi\left(\frac{y_i - \mathbf{x}_i^\top \boldsymbol{\beta}}{\sigma}\right) \right\}^{l_i}, \quad (22)$$

θ	Model	Standard Gaussian			Heteroskedastic			Gaussian Mixture		
		R^2	MAE	RMSE	R^2	MAE	RMSE	R^2	MAE	RMSE
All Test Data										
0.05	TL+ Σ	0.220	0.983	1.230	-0.500	1.205	1.558	0.528	0.766	0.957
	\mathcal{C} + Σ	0.499	0.793	0.986	-0.418	1.179	1.515	0.715	0.601	0.744
	\mathcal{C} +ELU	0.690	0.594	0.775	-0.376	1.159	1.493	0.744	0.555	0.705
0.50	TL+ Σ	0.904	0.346	0.433	0.904	0.351	0.432	0.909	0.336	0.421
	\mathcal{C} + Σ	1.000	0.015	0.018	1.000	0.015	0.018	1.000	0.014	0.017
	\mathcal{C} +ELU	0.990	0.069	0.141	0.987	0.096	0.156	0.989	0.090	0.149
0.95	TL+ Σ	0.979	0.156	0.200	0.811	0.855	1.035	0.974	0.176	0.222
	\mathcal{C} + Σ	0.985	0.137	0.172	0.913	0.412	0.703	0.983	0.153	0.183
	\mathcal{C} +ELU	0.973	0.184	0.230	0.947	0.374	0.547	0.982	0.155	0.185
Only Non-Censored										
0.05	TL+ Σ	0.135	0.443	0.591	-0.420	0.275	0.336	0.422	0.402	0.535
	\mathcal{C} + Σ	0.641	0.295	0.381	-0.441	0.279	0.339	0.585	0.347	0.453
	\mathcal{C} +ELU	0.742	0.246	0.323	-0.414	0.276	0.336	0.602	0.340	0.444
0.50	TL+ Σ	0.924	0.237	0.279	0.914	0.250	0.297	0.928	0.230	0.272
	\mathcal{C} + Σ	1.000	0.016	0.019	1.000	0.016	0.019	1.000	0.015	0.018
	\mathcal{C} +ELU	0.998	0.036	0.046	0.993	0.069	0.088	0.994	0.066	0.077
0.95	TL+ Σ	0.980	0.147	0.185	0.798	0.777	0.947	0.976	0.158	0.192
	\mathcal{C} + Σ	0.985	0.130	0.160	0.891	0.387	0.694	0.979	0.153	0.183
	\mathcal{C} +ELU	0.972	0.177	0.218	0.933	0.360	0.545	0.979	0.152	0.182

Table 2: Predictive quality for conditional quantiles of y^* in the synthetic datasets.

where φ is the Probability Density Function (PDF) of $\mathcal{N}(0, 1)$, Φ is its Cumulative Distribution Function (CDF), and for a given fixed threshold τ :

$$l_i = \begin{cases} 0, & y_i < \tau \\ 1, & y_i = \tau \end{cases}. \quad (23)$$

Let us now compare Tobit parametric modeling to non-parametric CQRNN, using the same synthetic baseline datasets as above. For both modeling methods, we use an NN with a single linear neuron, which we fit similarly to Section 4.1. When fitting Tobit, we fix $\sigma = 1$ and use the NLL of (22) as the loss function, whereas when fitting CQR for $\theta = 0.05, 0.95$, we use the NLL of (5) as the loss function.

Finally, we evaluate the performance via two common measures of Quantile Regression:

$$\text{ICP} = \text{fraction of } y^* \text{ within the estimated } 5\% - 95\% \text{ interval.} \quad (24)$$

$$\text{MIL} = \text{mean length of the estimated } 5\% - 95\% \text{ interval.} \quad (25)$$

ICP should be close to $0.95 - 0.05 = 0.9$, while MIL should converge to the latent MIL. Among models with same ICP, we thus prefer the one that yields the lowest MIL.

Table 3 on the following page summarizes the performance of Tobit and CQR. As expected, Tobit performs best on the synthetic dataset with Standard Gaussian noise, which most closely matches its modeling assumptions. When evaluated on all test observations, Tobit outperforms QR by obtaining ICP closer to the desired 0.9, for each synthetic dataset. However, when evaluated on just the non-censored test observations (approx. 30% of each dataset), where the true values are reliably known, QR outperforms Tobit while also maintaining ICP close to 0.9. The results thus suggest that CQRNN tends to yield flatter distributions (higher MIL) that better approximate the latent distribution of non-censored observations.

5 Experiments for Estimating Latent Mobility Demand

In this Section, we apply Censored Quantile Regression Neural Network (CQRNN) to real-world data from shared mobility services. Contrary to the synthetic datasets in the previous Section, real-world datasets do not feature the

Dataset	Model	All Test Data		Only Non-Censored	
		ICP	MIL	ICP	MIL
Standard Gaussian	Tobit	0.909	3.290	0.915	3.290
	$\mathcal{C} + \Sigma$	0.888	3.155	0.885	3.235
Heteroskedastic	Tobit	0.936	3.290	0.941	3.290
	$\mathcal{C} + \Sigma$	0.779	3.742	0.907	4.480
Gaussian Mixture	Tobit	0.852	2.601	0.852	2.601
	$\mathcal{C} + \Sigma$	0.721	2.644	0.907	3.081

Table 3: Non-parametric QR vs. parametric Tobit on synthetic datasets. Best ICP is highlighted in bold, and ties are broken by MIL.

latent variable. Hence similarly to (Gammelli et al., 2020), we treat the available data as y^* and manually censor it per various censorship schemes. We then fit several CQRNN models for $\theta = 0.05, 0.95$ and evaluate them via ICP (24) and MIL (25).

First, we use a censorship-unaware NN with a single linear unit (denoted as Σ), which we train to minimize plain Tilted Loss (18). Then, we equip the same architecture with censorship-awareness, using (5) as loss (denoted as \mathcal{C}). Thereafter, we experiment with non-linear activations, and finally add a Long Short-Term Memory (LSTM) (Hochreiter and Schmidhuber, 1997) in the Hidden layer, immediately before a linear Output Aggregation layer (Figure 1).

We also experiment with regularization (denoted as “Reg”) by letting the Dropout layer randomly eliminate 20% of the input and using ℓ_2 regularization in all subsequent layers. We have also experimented with either 1 or 10 stacked units with non-linear activations (tanh, sigmoid, ELU, RELU (Nielsen, 2015)) in the Hidden layer, either with or without regularization. However, these additional models performed poorly, as we further discuss in Section 6, and so we omit their results.

5.1 Bike-sharing Data

The first real-world dataset is obtained from Donkey Republic, a bike-sharing service provider in the Copenhagen metropolitan area in Denmark. The data consists of pickups and returns of bicycles in predefined hubs, which we aggregate spatially by “superhubs” and temporally by no. daily pickups daily, as in (Gammelli et al., 2020). superhubs rarely run out of bicycles at any moment, hence this data represents actual demand quite well.

We censor the data as follows:

1. Randomly select a γ portion of all y_i^* .
2. For each selected y_i^* , independently sample

$$\delta_i \sim \mathcal{U}[c_1, c_2], \tag{26}$$

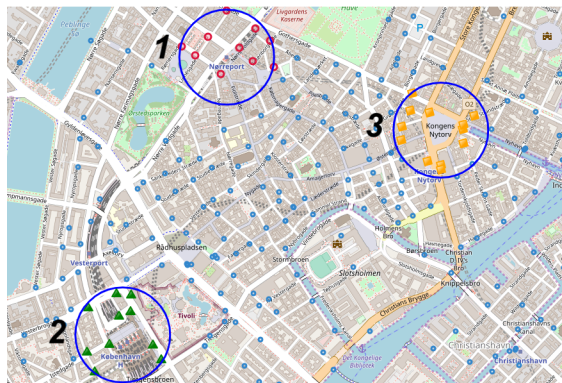
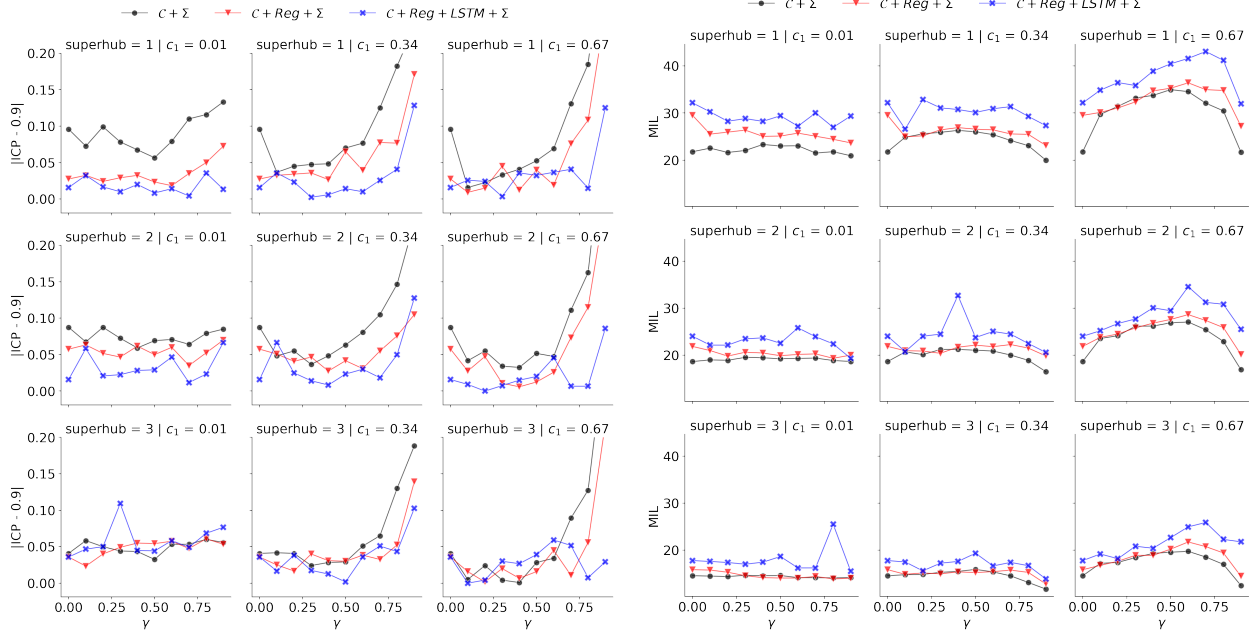
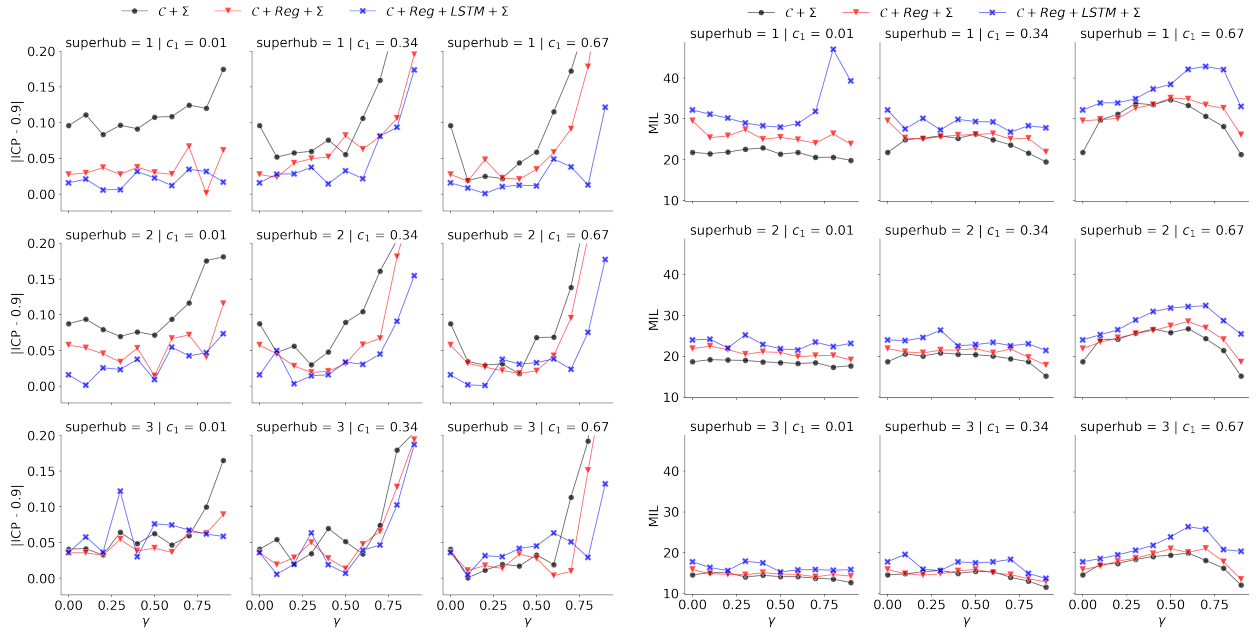


Figure 5: Bike-sharing hubs and aggregated superhubs, as in (Gammelli et al., 2020): 1) Nørreport, 2) Kgs. Nytorv, 3) København H.



(a) Mean $|ICP - 0.9|$ (left) and MIL (right) for bike-sharing data, evaluated on all test observations. Lower is better.



(b) Mean $|ICP - 0.9|$ (left) and MIL (right) for bike-sharing data, evaluated on non-censored test observations. Lower is better.

Figure 6: Results for bike-sharing data.

and let

$$y_i = (1 - \delta_i)y_i^*. \tag{27}$$

Our experiments use $\gamma = 0.0, 0.1, \dots, 0.9$ and $(c_1, c_2) = (0.01, 0.33), (0.34, 0.66), (0.67, 0.99)$. For each γ, c_1, c_2 , we independently censor the data 10 times to obtain differently censored datasets B_1, \dots, B_{10} , and we partition each B_j consecutively into train, validation and test sets with equal proportions. We then fit each NN model independently for 10 random initializations of weights, drawn independently from $\mathcal{N}(0, 1)$. The covariates are the 7 previous

observation lags, and the censorship thresholds for non-censored observations are

$$\tau_i^{(j)} = y_i^{(j)} \times \frac{\text{mean of train } y^*}{\text{mean of train } y^{(j)}}. \quad (28)$$

After fitting, we evaluate ICP and MIL for each γ, c_1, c_2 as follows. First, for each B_1, \dots, B_{10} , we consider only initializations that yield reasonable validation MIL, as:

$$\frac{\text{validation MIL}}{\text{mean of train } y^{(j)}} \leq 2. \quad (29)$$

We then select the initialization that yields validation ICP closest to 0.9. Finally, we average the test ICP and test MIL over the 10 selected initializations.

The results for the bike-sharing data experiments are summarized in Figure 6 on the previous page, both for the entire test set and for only non-censored test observations. To reduce visual clutter, we limit the vertical axis and omit results for non-regularized Σ with \mathcal{C} loss, as they are mostly worse than regularized Σ with \mathcal{C} . In each Figure, rows range over superhubs, columns range over (c_1, c_2) , and each horizontal axis ranges over γ . For ICP, we plot $|\text{ICP} - 0.9|$, namely, its distance from ideal ICP.

We see that a more complex architecture results in higher MIL, but also generally better ICP. The censorship-unaware model often yields the worst ICP, though as also found in (Gammelli et al., 2020), its ICP is occasionally better than that of the censorship-aware models, when relatively few observations are censored ($\gamma \leq 0.2$). The overall better performance of the censorship-aware models holds not only for the entire test set, but also for its non-censored subset, where the true (latent) values are known.

We also see that among CQRNN models, the LSTM-based model often yields better ICP than the purely linear model. An exception to this is the case of superhub 3 with $(c_1, c_2) = (0.67, 0.99)$, where the linear CQRNN yields the best ICP on both test subsets, possibly because this more challenging case requires better fitting of LSTM weights.

5.2 Shared Electric Vehicles Data

The second real-world dataset comes from Share Now, a shared Electric Vehicles (EVs) service operator in the Copenhagen metropolitan area too. The EVs are picked up from and returned to reserved parking areas. This dataset, which we denote as \mathcal{D}_{EV} , consists of 2.6 million trips in years 2016-2019, where each trip record contains the endpoints, driver ID and vehicle ID.

We wish to experiment with complete censorship of daily demand of EV mobility. First, we let y_1^*, \dots, y_N^* be the daily no. trip starts in \mathcal{D}_{EV} . For censorship, we use the following scheme:

1. Randomly select an α portion of all vehicles in \mathcal{D}_{EV} .
2. Let \mathcal{D}'_{EV} be \mathcal{D}_{EV} without any trips that involve the selected vehicles.
3. Let y_1, \dots, y_N be the daily no. trip starts in \mathcal{D}'_{EV} .

Consequently, every y_i is censored, so that

$$y_i \approx (1 - \alpha)y_i^*, \quad (30)$$

as illustrated in Figure 7 on the following page.

Because all observations are censored, there is no need to specify any threshold for non-censored observations. For each $\alpha = 10\%, 20\%, 30\%, 40\%$, we independently apply the censorship scheme 10 times. For each of the 10 censored datasets thus obtained, we partition into train:validation:test as 1 : 1 : 1 and fit each NN with random initialization of weights, drawn independently from $\mathcal{N}(0, 1)$. Finally, we evaluate each NN by averaging its test ICP and test MIL over the 10 experiments.

The results appear in Table 4 on the next page, where we see that the censorship-unaware model mostly yields both the worst ICP and worst MIL. Regularization again improves results for the censorship-aware Σ with \mathcal{C} loss. Among the censorship-aware models, the LSTM model often yields the best ICP, and otherwise has ICP close to the ICP of the regularized linear model. For censorship-aware models too, better ICP is accompanied by higher MIL, as in Section 5.1. As expected in complete censorship, all models deteriorate rapidly as α increases and yield ICP far below 0.9 for $\alpha = 0.4$, where our experiments thus stop.

Model	$\alpha = 10\%$		$\alpha = 20\%$		$\alpha = 30\%$		$\alpha = 40\%$	
	ICP	MIL	ICP	MIL	ICP	MIL	ICP	MIL
TL Σ	0.870 \pm 0.0	1680 \pm 123	0.659 \pm 0.0	1442 \pm 75	0.341 \pm 0.1	1339 \pm 84	0.106 \pm 0.0	1105 \pm 62
C Σ	0.858 \pm 0.0	1594 \pm 59	0.673 \pm 0.0	1419 \pm 64	0.342 \pm 0.1	1242 \pm 74	0.127 \pm 0.0	1084 \pm 107
C Reg+ Σ	0.912 \pm 0.0	2017 \pm 68	0.858 \pm 0.0	1848 \pm 84	0.683 \pm 0.1	1641 \pm 109	0.282 \pm 0.1	1406 \pm 48
C LSTM+ Σ	0.904 \pm 0.0	2210 \pm 165	0.850 \pm 0.1	2014 \pm 262	0.779 \pm 0.1	2329 \pm 1114	0.343 \pm 0.2	1595 \pm 302

Table 4: Results of experiments with shared EV data, as average \pm standard deviation. Best ICP is highlighted in bold.

6 Conclusion

In this work, we propose to estimate the full distribution of latent mobility demand via Censored Quantile Regression Neural Networks (CQRNN). First, we demonstrate the advantages of CQRNN using synthetic baseline datasets with various noise distributions, both homoskedastic and heteroskedastic. We obtain that CQRNN outperforms censorship-unaware QRNN on both the entire test set and its non-censored subset, where the true values are reliably known. We also compare CQRNN to the common Tobit model, which assumes Gaussian white noise, and obtain that CQRNN tends to yield flatter distributions that better approximate the latent uncertainty structure of non-censored observations.

Next, we apply CQRNN to real-world datasets from two shared mobility services – bike-sharing and shared Electric Vehicles (EVs) – which we randomly censor either partially or completely. For both datasets, more complex CQRNN architectures yield higher MIL and generally better ICP – where the use of Long Short-Term Memory (LSTM) often leads to best performance – whereas censorship-unaware QRNN often yields the worst ICP.

The experiments on synthetic and real-world dataset thus lead to similar conclusions about the effectiveness of CQRNN for Censored Regression. One difference, however, is that the use of nonlinear activations improves performance for the synthetic datasets, yet deteriorates performance for the real-world datasets. The cause for this is unlikely to be overfitting, as we use regularization techniques. Instead, a possible cause is the non-differentiability of our censored loss function, which may thus benefit from smoothing as in (Cannon, 2011).

For future work, we therefore plan to experiment with a smooth approximation of the loss function. We also plan to experiment with multivariate Quantile Regression, e.g., similarly to (Rodrigues and Pereira, 2020). Further, we plan to take advantage of possible spatio-temporal correlations in the datasets, e.g., using Convolutional Neural Networks as in (Chu et al., 2019).

References

Moshe Buchinsky. Recent advances in quantile regression models: a practical guideline for empirical research. *Journal of human resources*, pages 88–126, 1998.

Alex J Cannon. Quantile regression neural networks: Implementation in r and application to precipitation downscaling. *Computers & geosciences*, 37(9):1277–1284, 2011.

Guillaume Carlier, Victor Chernozhukov, Alfred Galichon, et al. Vector quantile regression: an optimal transport approach. *The Annals of Statistics*, 44(3):1165–1192, 2016.

Colin Chen. A finite smoothing algorithm for quantile regression. *Journal of Computational and Graphical Statistics*, 16(1):136–164, 2007.

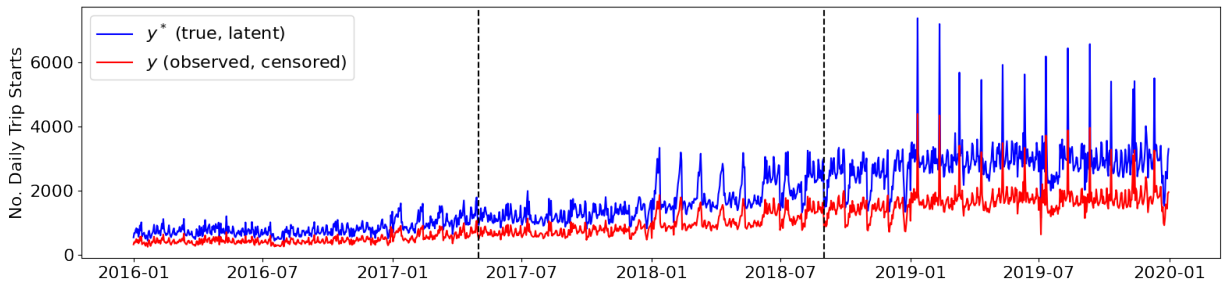


Figure 7: Shared EV data and $\alpha = 40\%$ fleet reduction.

- Jung-Yu Cheng and Shinn-Jia Tzeng. Quantile regression of right-censored length-biased data using the buckley–james-type method. *Computational Statistics*, 29(6):1571–1592, 2014.
- Victor Chernozhukov, Iván Fernández-Val, and Amanda E Kowalski. Quantile regression with censoring and endogeneity. *Journal of Econometrics*, 186(1):201–221, 2015.
- Kai-Fung Chu, Albert YS Lam, and Victor OK Li. Deep multi-scale convolutional lstm network for travel demand and origin-destination predictions. *IEEE Transactions on Intelligent Transportation Systems*, 2019.
- Antonio F. Galvao, Carlos Lamarche, and Luiz Renato Lima. Estimation of censored quantile regression for panel data with fixed effects. *Journal of the American Statistical Association*, 108(503):1075–1089, 2013. doi: 10.1080/01621459.2013.818002.
- Daniele Gammelli, Inon Peled, Filipe Rodrigues, Dario Pacino, Haci A. Kurtaran, and Francisco C. Pereira. Estimating latent demand of shared mobility through censored gaussian processes. *Transportation Research Part C: Emerging Technologies*, 120, 2020. doi: 10.1016/j.trc.2020.102775.
- Ali Gannoun, Jérôme Saracco, Ao Yuan, and George E Bonney. Non-parametric quantile regression with censored data. *Scandinavian Journal of Statistics*, 32(4):527–550, 2005.
- Stephen Haben and Georgios Giasemidis. A hybrid model of kernel density estimation and quantile regression for gefcom2014 probabilistic load forecasting. *International Journal of Forecasting*, 32(3):1017–1022, 2016.
- Yaoyao He and Haiyan Li. Probability density forecasting of wind power using quantile regression neural network and kernel density estimation. *Energy conversion and management*, 164:374–384, 2018.
- Yaoyao He and Wanying Zhang. Probability density forecasting of wind power based on multi-core parallel quantile regression neural network. *Knowledge-Based Systems*, 209:106431, 2020.
- Yaoyao He, Yang Qin, Shuo Wang, Xu Wang, and Chao Wang. Electricity consumption probability density forecasting method based on lasso-quantile regression neural network. *Applied energy*, 233:565–575, 2019.
- Veli Himanen, Peter Nijkamp, and Aura Reggiani. *Neural networks in transport applications*. Routledge, 2019.
- Sepp Hochreiter and Jürgen Schmidhuber. Long short-term memory. *Neural computation*, 9(8):1735–1780, 1997.
- Yichen Jia and Jong-Hyeon Jeong. Deep learning for quantile regression: Deepquantreg, 2020.
- Diederik P Kingma and Jimmy Ba. Adam: A method for stochastic optimization. *arXiv preprint arXiv:1412.6980*, 2014.
- Roger Koenker. *Quantile Regression*. Econometric Society Monographs. Cambridge University Press, 2005. doi: 10.1017/CBO9780511754098.
- Roger Koenker and Gilbert Bassett. Regression quantiles. *Econometrica: journal of the Econometric Society*, pages 33–50, 1978.
- Roger Koenker and Beum J Park. An interior point algorithm for nonlinear quantile regression. *Journal of Econometrics*, 71(1-2):265–283, 1996.
- Gilbert Laporte, Frédéric Meunier, and Roberto Wolfler Calvo. Shared mobility systems: an updated survey. *Annals of Operations Research*, 271(1):105–126, 2018.
- Chenlei Leng and Xingwei Tong. A quantile regression estimator for censored data. *Bernoulli*, 19(1):344–361, 2013. doi: 10.3150/11-BEJ388.
- Alexander Hanbo Li and Jelena Bradic. Censored quantile regression forest. In *International Conference on Artificial Intelligence and Statistics*, pages 2109–2119. PMLR, 2020.
- Thomas A Mroz. The sensitivity of an empirical model of married women’s hours of work to economic and statistical assumptions. *Econometrica: Journal of the econometric society*, pages 765–799, 1987.
- Michael A Nielsen. *Neural networks and deep learning*, volume 2018. Determination press San Francisco, CA, 2015.
- Inon Peled, Kelvin Lee, Yu Jiang, Justin Dauwels, and Francisco Camara Pereira. Preserving uncertainty in demand prediction for autonomous mobility services. In *Proceedings of the IEEE Intelligent Transportation Systems Conference (ITSC) 2019*, pages 3043–3048, United States, 2019. IEEE. doi: 10.1109/ITSC.2019.8916878.
- James L Powell. Least absolute deviations estimation for the censored regression model. *Journal of Econometrics*, 25(3):303–325, 1984.
- James L Powell. Censored regression quantiles. *Journal of econometrics*, 32(1):143–155, 1986.
- V.A. Profillidis and G.N. Botzoris. Chapter 3 - methods of modeling transport demand. In V.A. Profillidis and G.N. Botzoris, editors, *Modeling of Transport Demand*, pages 89 – 123. Elsevier, 2019. doi: 10.1016/B978-0-12-811513-8.00003-0.

- Joaquin Quiñonero-Candela, Carl Edward Rasmussen, Fabian Sinz, Olivier Bousquet, and Bernhard Schölkopf. Evaluating predictive uncertainty challenge. In Joaquin Quiñonero-Candela, Ido Dagan, Bernardo Magnini, and Florence d'Alché Buc, editors, *Machine Learning Challenges. Evaluating Predictive Uncertainty, Visual Object Classification, and Recognising Textual Entailment*, pages 1–27, Berlin, Heidelberg, 2006. Springer Berlin Heidelberg. doi: 10.1007/11736790_1.
- Filipe Rodrigues and Francisco C Pereira. Beyond expectation: deep joint mean and quantile regression for spatiotemporal problems. *IEEE Transactions on Neural Networks and Learning Systems*, 2020.
- Georgina Santos. Sustainability and shared mobility models. *Sustainability*, 10(9):3194, 2018.
- Jooyong Shim and Changha Hwang. Support vector censored quantile regression under random censoring. *Computational statistics & data analysis*, 53(4):912–919, 2009.
- Göran Smith and David A Hensher. Towards a framework for mobility-as-a-service policies. *Transport policy*, 89: 54–65, 2020.
- Nitish Srivastava, Geoffrey Hinton, Alex Krizhevsky, Ilya Sutskever, and Ruslan Salakhutdinov. Dropout: a simple way to prevent neural networks from overfitting. *The journal of machine learning research*, 15(1):1929–1958, 2014.
- James W Taylor. A quantile regression neural network approach to estimating the conditional density of multiperiod returns. *Journal of Forecasting*, 19(4):299–311, 2000.
- Wen Tian, Jinjin Song, Yixing Guo, and Fan Yang. Probabilistic airport traffic demand prediction incorporating the weather factors. In *Journal of Physics: Conference Series*, volume 1510, page 012022, 2020.
- James Tobin. Estimation of Relationships for Limited Dependent Variables. *Econometrica*, 26(1):24–36, 1958. ISSN 00129682, 14680262. URL <http://www.jstor.org/stable/1907382>.
- Yunwen Yang, Huixia Judy Wang, and Xuming He. Posterior inference in bayesian quantile regression with asymmetric laplace likelihood. *International Statistical Review*, 84(3):327–344, 2016.
- Keming Yu and Julian Stander. Bayesian analysis of a Tobit quantile regression model. *Journal of Econometrics*, 137(1):260–276, 2007. ISSN 03044076. doi: 10.1016/j.jeconm.2005.10.002.
- Wenjie Zhang, Hao Quan, and Dipti Srinivasan. An improved quantile regression neural network for probabilistic load forecasting. *IEEE Transactions on Smart Grid*, 10(4):4425–4434, 2018.
- Songfeng Zheng. Qboost: Predicting quantiles with boosting for regression and binary classification. *Expert Systems with Applications*, 39(2):1687–1697, 2012.